DOI: 10.13009/EUCASS2025-291
11TH EUROPEAN CONFERENCE FOR AERONAUTICS AND SPACE SCIENCES (EUCASS)

Evaluation of TNT Equivalence of Launch Vehicle Fuel (LOX/LCH4) by 1kg-Class Explosion Experiment

Shungo Okamura [1†], Tetsuya Fujiwara [1], Atsushi Ikemoto [1], Keita Yamamoto [1], Tei Saburi [2] and Shu Usuba [2]
[1] Japan Aerospace Exploration Agency (JAXA)
Tsukuba, Ibaraki, 305-8505, Japan
[2] National Institute of Advanced Industrial Science and Technology (AIST)
Tsukuba, Ibaraki, 305-8569, Japan
okamura.shungo@jaxa.jp – fujiwara.tetsuya@jaxa.jp – ikemoto.atsushi@jaxa.jp – yamamoto.keita@jaxa.jp – t.saburi@aist.go.jp – s-usuba@aist.go.jp
[†] Corresponding Author

Abstract
1kg-class explosion experiment with LOX/LCH4 was conducted to contribute to the determination of safety distances for LOX/LCH4-fueled launch vehicle, and the results showed that the TNT equivalence of approximately 1 ~ 10%. This paper details the unique experimental method, presents the results, and discusses the correlation between the mixing ratio and TNT equivalence and heat radiation data obtained.

1. Introduction

In recent years, liquid methane (LCH4) has become one of the major fuels for launch vehicles. Notable examples include the Raptor by SpaceX and the BE-4 by Blue Origin, both well-known methane engines, as well as JAXA's LE-8, an LNG engine primarily composed of methane. CH4 features higher boiling point and density compared to liquid hydrogen (LH2), which confers benefits in terms of fuel storability and accessibility. Furthermore, it enables a reduction in launch vehicle weight by allowing for decreased fuel tank sizes. Despite these advantages, a comprehensive safety standard for launch vehicles using liquid oxygen (LOX)/LCH4 has not yet been fully established. This gap is primarily attributed to an insufficient understanding of characteristics of LOX/LCH4 explosions.
To establish safety regulations for launch site operations [1] involving new fuels, the launch site's safety distance is crucial. Criteria for determining this distance are typically based on blast pressure, fragments and debris, and heat radiation from the fireball, and are calculated primarily by using TNT equivalence. It is a scale factor comparing the explosive power of the targeted fuel to that of TNT whose explosive power is well-established [2-6], and often adopted as an indicator of explosive strength. For instance, JAXA, in collaboration with NASA [7], has experimentally measured the TNT equivalence of LOX/LH2, which contributed to current safety standard for launch site operations [1]. JAXA also experimentally measured the TNT equivalence of LOX/LNG during the development of the LNG engine [8]. However, information regarding the scale effect of weight and the influence of mixing ratio on TNT equivalence is limited and not well-investigated [9-11].
Given these circumstances, JAXA is researching the safety distance of LOX/LCH4 at launch sites. The goal is to establish safety standards for LCH4-fueled launch vehicles by clarifying how fuel mass, mixing ratio, and other factors influence TNT equivalence. This paper presents the results of LOX/LCH4 1kg-class explosion experiments conducted at the JAXA Noshiro Rocket Testing Center, serving as a crucial first step in the TNT equivalence of LCH4 explosions.

2. Experimental Setup

2.1 Objective of the experiment

The main objective of the experiments is to evaluate the TNT equivalence of LCH4, specifically targeting the situation 'impact mode' [12]. Impact mode describes a scenario where a launch vehicle loses thrust for some reason immediately after liftoff, falls to the ground and explodes before a self-destruct command can be issued. To simulate this, two glass dewars, respectively filled with LOX and LCH4, are dropped from a certain height and exploded upon impact with the ground (Figure 1). This method is based on the previous experiment [8]. As indicated by a previous study [8], self-

DOI: 10.13009/EUCASS2025-291

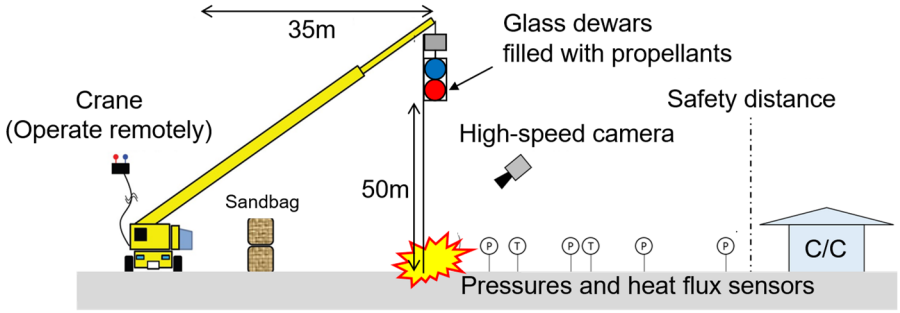

Figure 1: Schematic of the explosion experiment

Figure 2: Experimental Field
(JAXA Noshiro Rocket Testing Center)

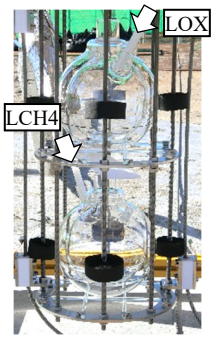

Figure 3: Glass dewars

ignition was expected to occur immediately after impact; therefore, the experiment proceeded under this assumption. In this experiment, blast pressure and heat radiation were measured to evaluate the explosive power of 1 kg-class LOX/LCH4.

2.2 Experimental method

The glass dewars' drop height is set to be 50 m to achieve an impact velocity of approximately 30 m/s. For safety, the crane was operated remotely to lift and drop the dewars. This experiment took place at the JAXA Noshiro Rocket Testing Center (Figure 2), following this procedure:

1. Place the vessel at the explosion point and insert a flexible hose for propellant filling.
2. Remotely fill the vessel with fuel and withdraw the flexible hose.
3. Lift the vessel to a height of 50 m using a crane.
4. Drop the vessel.

To simulate actual launch site conditions, concrete was placed at the point of explosion, and the vessel was dropped through guide wires to ensure that it fell at the intended location. All procedures from step 2 onward were designed for remote execution from the control center (C/C). In this experiment, spherical adiabatic glass dewars were used to focus on the mixing behavior of LOX/LCH4 and minimize the effects of the fuel vessel's shape and material. Assuming the fuel arrangement in a launch vehicle, the LOX-filled and LCH4-filled glass dewars were positioned in upper and lower positions, respectively (Figure 3).

2.2 Experimental Measurement

Figure 4 illustrates the arrangement of measurement devices. As for ground conditions, while concrete was set at the explosion point, other areas (the white areas in Figure 4) consisted of sandy ground. Blast pressures and heat radiations are measured at various points located up to 175 m away from the explosion. For pressure measurement, blast impact sensors (PCB 113B28, sensitivity 14.5 mV/kPa) were placed within a range of 3 m ~ 150 m from the explosion point.

DOI: 10.13009/EUCASS2025-291

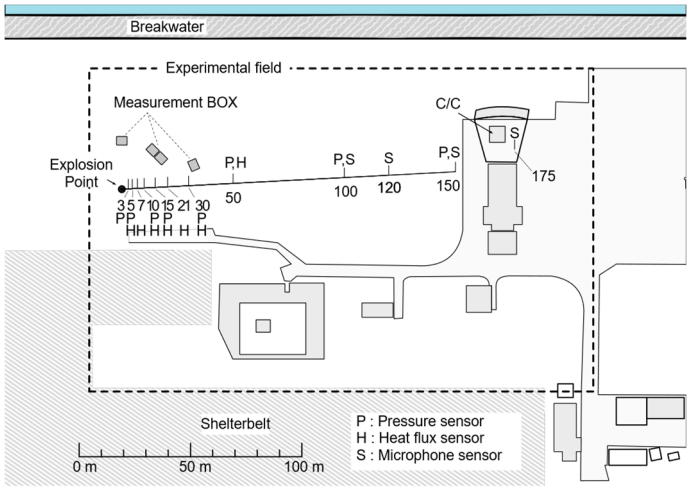

Figure 4: Arrangement of measurement devices

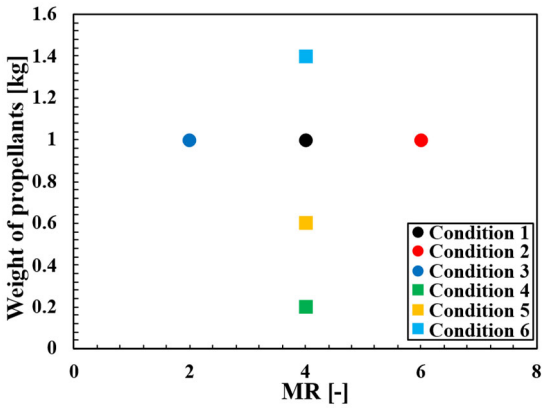

Figure 5: Target weight of Propellants and MR

To account for pressure decay at greater distances, sound pressure sensors (PCB 378C10, sensitivity 1.0 mV/kPa) were additionally placed at distances ranging from 100 m ~ 175 m. Heat radiation was measured by using heat flux sensors (CAPTEC RF-50: 50mm x 50mm, rated 5 μV/W/m^2) positioned 5 m to 50 m from the explosion point. For video observation, measurement boxes were placed at 20 m from the explosion point. These boxes protected the high-speed cameras (Phantom T-1340, TMX6410) and normal- speed video cameras from weather, blast effects and flying debris. The captured images were used to analyze the impact velocity, explosion behavior and flame width. To verify the accuracy of the measurements, the ground surface explosion experiment using C-4, a material with a well-known TNT equivalence, were also conducted.

2.3 Experimental condition

The target weight of propellants and mixing ratio (MR) were set as shown in Figure 5. This experiment aimed to determine two key parameter dependencies:

- Correlation between MR and TNT equivalence: We fixed the total weight of propellants weight at 1 kg and varied the MR from 2 to 6.
- Scale effect of propellant weight on TNT equivalence: We fixed the MR at 4 (equivalent ratio) and varied the total propellant weight from 0.2 kg to 1.4 kg.

To confirm reproducibility, experiments were conducted twice for each planned condition.

3. Results and Discussions

Figures 6 displays the actual weight of propellants just before drop-off. This weight was calculated using the following method.

- First, the weight immediately after fuel filling was determined by observing the liquid level in the dewar with a camera.
- Then, the final weight at the drop-off was calculated using pre-measured evaporation rate data.

The actual weight varied slightly from the target because remotely controlling the exact amount of propellant filled into the dewar proved challenging.

Figure 7 presents the sample images from the explosions. In total, 12 experiments were conducted, and the explosions occurred in 10 cases. In the remaining two cases (No. 2 and No. 8), no explosion occurred. In all cases where explosion occurred, the fuel self-ignited simultaneously with impact. This self-ignition was also observed in previous experiments [8], suggesting the same ignition mechanism likely occurred in this experiment. We attempted to capture the self-ignition process with a high-speed camera to observe the moment of explosion, but the ignition source was obscured by the vapor cloud (figure omitted), preventing direct observation. The precise mechanism of self-ignition is currently under evaluation. The causes of non-explosions in cases No. 2 and No. 8 were investigated by examining the impact velocity and angle but found no clear reason. Additionally, heat radiation data for No. 5 and No. 12 could not be measured properly. This was due to data exceeding the sensor's measurement range in one instance and the heat flux sensor measurement trigger not being detected in the other.

DOI: 10.13009/EUCASS2025-291

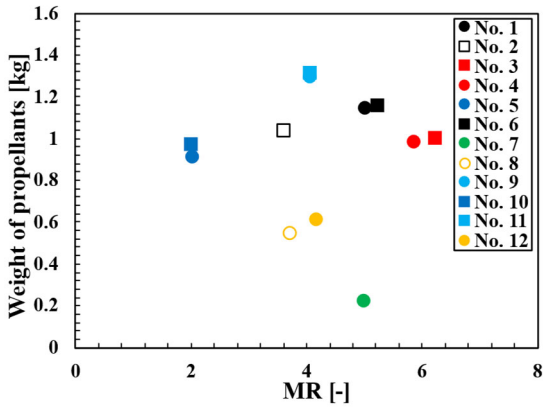

Figure 6: Actual weight of propellants and MR

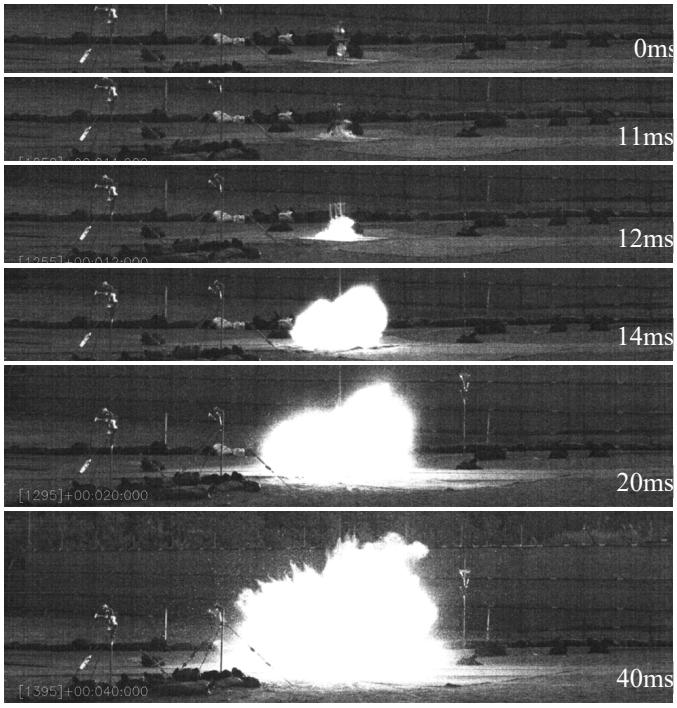

Figure 7: Sample of the explosion image captured by a high-speed camera (No. 6)

3.1 Pressure and heat radiation results

Figures 8 and 9 display samples of measured blast pressure and heat radiation data, respectively. Figure 8 shows that a characteristic pressure spike and rapid decay were captured at each measurement point upon arrival of the blast pressure, validating the measurements. The measurements at 3 m and 5 m exhibit noisy behavior after the initial pressure decay. Since this noise was not present in the C-4 explosion (figure omitted), it is attributed to flying glass debris from the dewar impacting the blast pressure sensor. The overall noise in Figure 8(b) likely stems from amplifier magnification or the effect of the long BNC measurement cable. Figure 8(c) illustrates the relationship between peak overpressure and distance, showing a clear trend of peak overpressure decaying with increasing distance from the explosion point.

Figure 9(a) demonstrates that, due to the high speed of radiation transmission, heat radiation detection at each measurement position was almost simultaneous. Figure 9(b) indicates that peak heat radiation tended to decrease with distance from the explosion point. It is important to note, however, that the heat flux sensor (CAPTEC RF-50) has a response time of 0.05 [s].

3.2 TNT equivalence

Figure 10 presents the peak overpressure and scaled impulse computed from integrating pressure over time with respect to the scaled distance. The solid lines in Figure 10 represent reference curves for typical ground surface explosions using TNT [6, 13]. While pressure was measured up to 175 m from the explosion point, the TNT equivalence should be computed within the range defined by the reference curve [13]. Therefore, the peak overpressure and scaled impulse were evaluated using measured values up to 198.5 m/kg$^{1/3}$ and 158.7 m/kg$^{1/3}$, respectively. In this study, the TNT equivalence is computed as follows:

$$TNT_{eq} = \frac{W_{TNT}}{W_p} \tag{1}$$

where TNT_{eq}, W_{TNT}, and W_p represent the TNT equivalence, the equivalent weight of TNT and the weight of propellants, respectively. In this experiment, the TNT equivalence was computed by fitting measurement data to the reference curve, substituting W_p with $W_{TNT} = (TNT_{eq} \cdot W_p)$. The results from C-4 experiments, which have a known TNT equivalence, showed a similar trend to the reference curve. This demonstrates the accuracy of blast pressure measurements with the current setup. It is important to note that the C-4 results were scaled using its already established

DOI: 10.13009/EUCASS2025-291

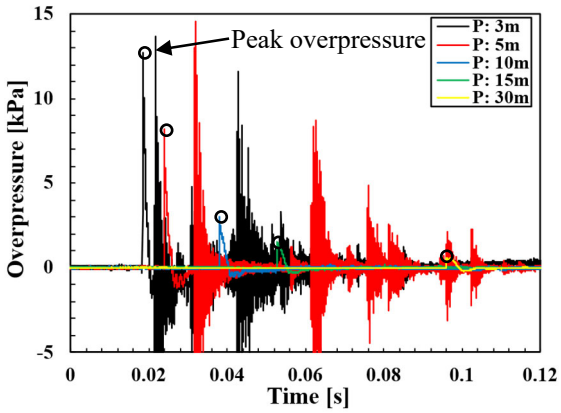

(a) Overpressure (3m ~ 30 m)

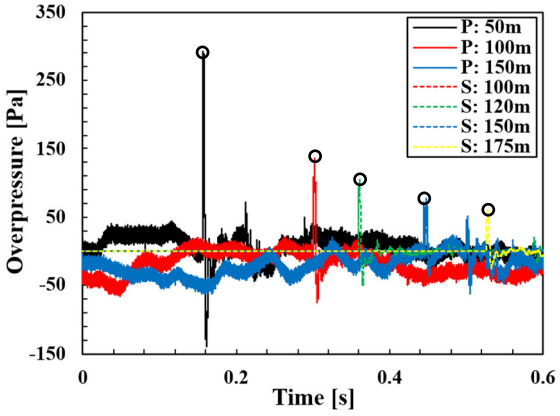

(b) Overpressure (50m ~ 175 m)

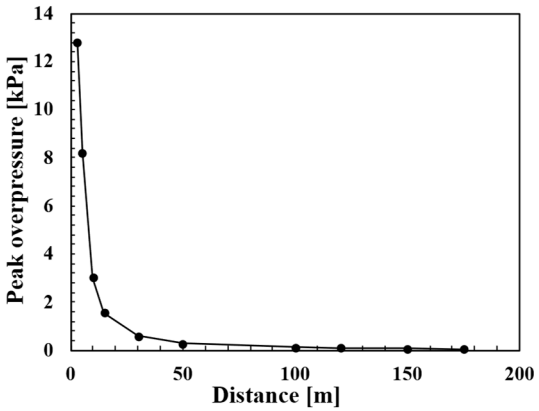

(c) Relationship between peak overpressure and distance

Figure 8: Sample of pressure signal (No. 6)

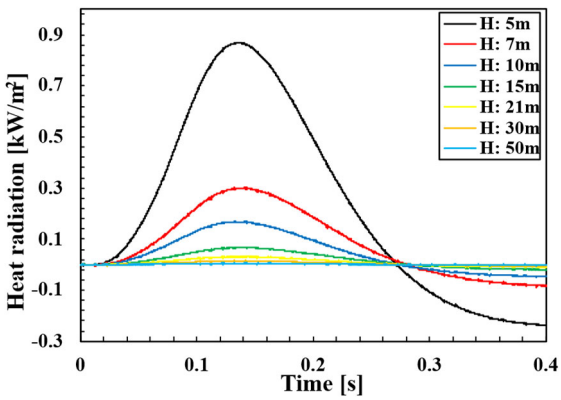

(a) Time characteristics of heat radiation

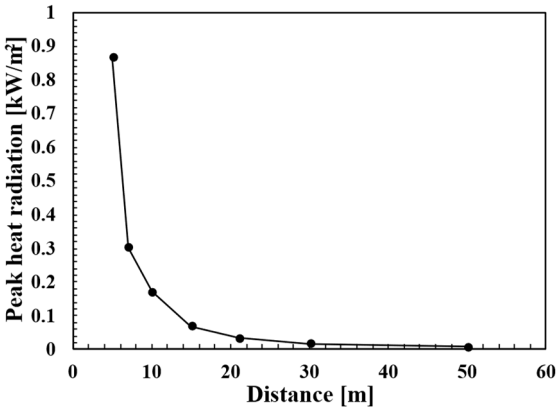

(b)Relationship between peak heat radiation and distance

Figure 9: Sample of heat radiation signal (No. 6)

TNT equivalence (137% for peak overpressure and 119% for scaled impulse) [14]. For each case, the TNT equivalence obtained by fitting the measured values to the reference curve using the least squares method was 1.1 ~ 6.8% for peak overpressure and 2.4 ~ 7.5% for scaled impulse.

Figure 11(a) and (b) illustrate the relationship between distance and TNT equivalence based on peak overpressure and scaled impulse, respectively. Figure 11(a) reveals that the TNT equivalence derived from peak overpressure varies significantly with distance. The same trend is observed in C-4 experiments (figure omitted), suggesting this variability is likely influenced by the experimental environment. In contrast, Figure 11(b) shows that the TNT equivalence based on scaled impulse exhibits little variation with distance. Consequently, we used TNT equivalence based on scaled impulses to evaluate the data from this experiment. Regarding Figure 11(b), the TNT equivalence for Case No. 4 is notably higher than in other cases. Since Case No. 4's conditions were almost identical to those of Case No. 3, and only Case No. 4 recorded a higher blast pressure, we believe this is not due to the influence of specific parameters, but

DOI: 10.13009/EUCASS2025-291

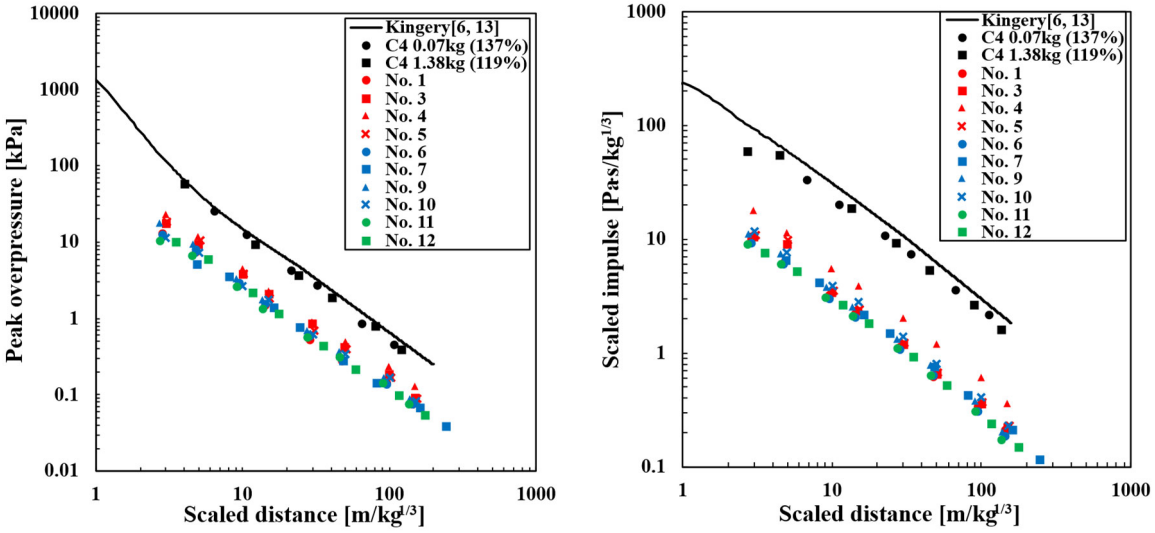

(a) Peak overpressure (b) Scaled impulse

Figure 10: Relationship between scaled distance and blast pressure

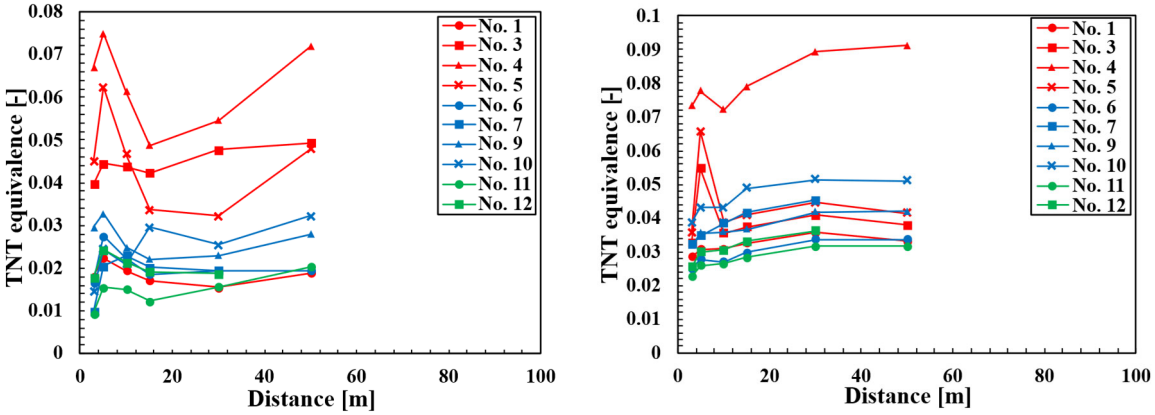

(a) Peak overpressure (b) Scaled impulse

Figure 11: TNT equivalence for each measurement point

rather a unique phenomenon. However, we have not yet identified the cause of the phenomenon, and it requires careful future evaluation.

3.3 Flame propagation speed

In this section, we evaluate whether the explosion was a detonation or a deflagration based on its flame propagation speed. The flame propagation speed was estimated from images captured by the high-speed camera. Figure 12(a) illustrates the time variation of flame width and height in Experiment No. 1, with the moment of vessel impact set as 0 s. The flame's width and height are values converted from pixels using a pre-captured calibration image (5 m = 952.84 pixels). Figure 12(b) shows the time variation of the flame propagation speed, computed using forward differences based on data in Figure 12(a) with a time increment of 0.0002 s. As seen in Figure 12(b), the maximum flame propagation speed was approximately 500 m/s immediately after the explosion. This speed is significantly lower than the detonation velocity (2300 m/s) for a premixed methane/oxygen gas. Therefore, the flame propagation speed computed via image analysis revealed no evidence of detonation. The flame propagation speed was consistent across other cases, leading us to presume that detonation did not occur in any of the experiments.

DOI: 10.13009/EUCASS2025-291

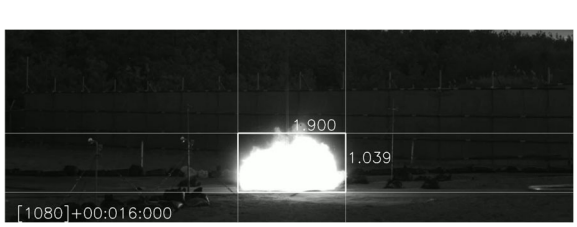

(i)

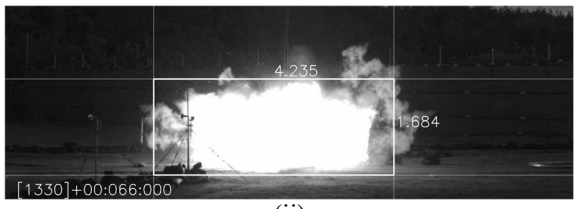

(ii)

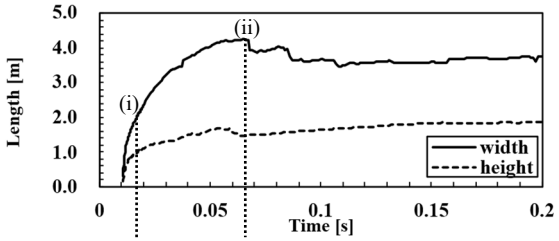

(a) Time variation of flame width and height

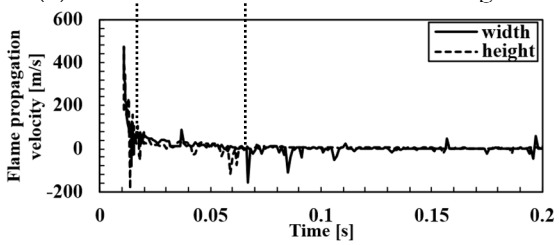

(b) Time variation of flame propagation speed

Figure 12: Sample of the time profile of frame (No. 1)

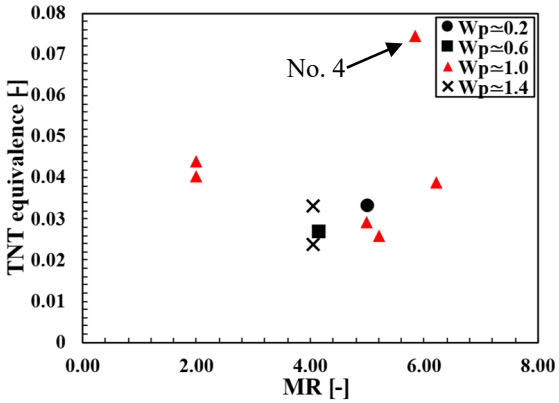

(a) MR dependence

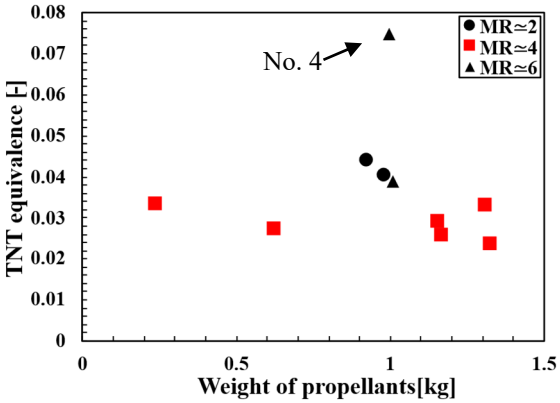

(b) Scale effect of the weight

Figure 13: The MR dependence and the scale effect of propellants weight

3.4 Effects of experimental parameters on TNT equivalence

3.4.1 Effect of MR and weight of propellants

We evaluated the MR dependence and the scale effect of propellant weight, which were the primary objectives of the experiment (section 2.3). The results of the evaluation are presented in Figure 13. While Example No. 4 exhibited a unique phenomenon, as noted in section 3.2, its data is included for reference.

Figure 13(a) illustrates the relationship between TNT equivalence and MR. Focusing on conditions where $W_p \cong 1.0$, it appears that the TNT equivalence tends to decrease around MR $= 4$. This result might reflect the MR dependence of the explosion energy. Figure 13(b) shows the relationship between weight of propellants and TNT equivalence. Focusing on conditions where MR $\cong 4$, no significant scale effect was obtained within the range of propellant weights used in this experiment. While some report indicate that yield decreases as weight of propellants increases in full-scale explosions [15], this tendency was not apparent in this experiment. We believe this is because the range of propellant weight variation in our experiment was relatively small.

However, it is crucial to note that these results are influenced by various parameters, such as the behavior of the glass dewar's destruction. The total weight of propellants in the experiment was approximately 1 kg, and the momentum or kinetic energy of the impact was comparable to, or even less than that of the glass dewars themselves (about 0.8 kg per dewar). Consequently, the dispersal and mixing behavior of the propellants at impact are likely significantly affected by the destruction process of the glass dewar.

DOI: 10.13009/EUCASS2025-291

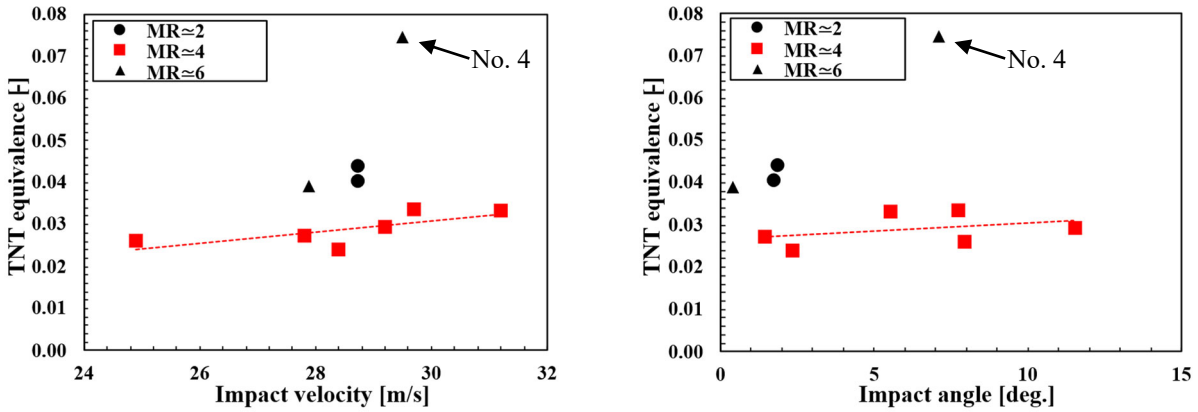

(a) Impact velocity (b) Impact angle

Figure 14: The effect of the impact velocity and angle

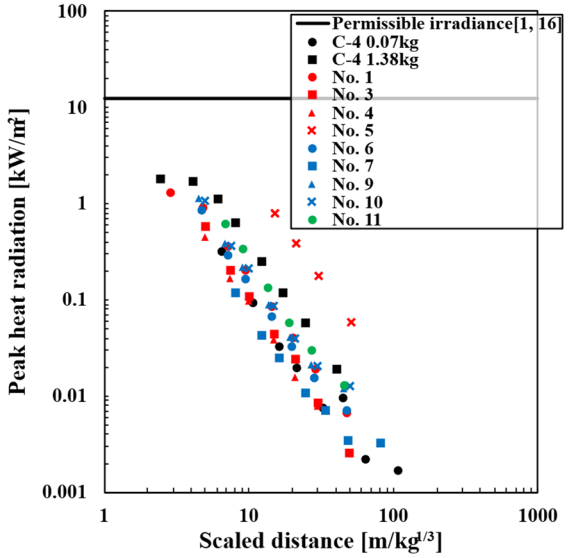

Figure 15: Relationship between scaled distance and peak heat radiation

3.4.2 Effect of other parameters

Figure 14 illustrates the effects of impact velocity and angle on TNT equivalence. As mentioned above, Case No. 4 serves as a reference point. Since we found a slightly higher MR sensitivity in Section 3.4.1, the data in Figure 14 is classified by MR. For MR ≅ 4, where wide range of data were obtained, approximate straight lines were drawn.
Figure 14(a) indicates a slight tendency for TNT equivalence to increase with increasing impact velocity. This aligns with previous reports suggesting that explosion power increases with impact velocity [11]. However, we should interpret the results carefully because the range of impact velocities in this study was relatively small. Figure 14(b) shows that the TNT equivalence slightly increases as the impact angle increases. This was contrary to our expectations. It had been anticipated that the TNT equivalence would increase as the impact angle decreased, as a smaller angle should allow for better propellant mixing.
As discussed in Section 3.4.1, it is important to note that various parameters, including the destruction behavior of the glass dewars, influence these results. We believe a more representative trend could be observed by increasing weight of propellant to a point where the dewar's destruction behavior becomes negligible.

3.5 Heat radiation

Figure 15 illustrates the relationship between scaled distance and peak heat radiation. Notably, the peak heat radiation measured in this study was below the permissible irradiance of 12.56 kW/m^2 according to technical standards [1, 16] in all cases. However, Case No. 5 exhibited significantly higher peak heat radiation compared to other cases. Given

DOI: 10.13009/EUCASS2025-291

that the heat radiation was measured under the same conditions as those of No. 5 in No. 10, we suspect a unique phenomenon occurred in Case No. 5 rather than the influence of specific parameters. The cause of this phenomenon remains unidentified and warrants further careful evaluation.

4. Conclusion

In this study, 1kg-class explosion experiment using LOX/LCH4 was conducted, and the following remarks are obtained.

- The experimental method for dropping and exploding LOX/LCH4 was established, obtaining valid data.
- While TNT equivalence based on peak overpressure varied with distance, the scaled impulse-based TNT equivalence proved robust against measured pressure data. This scaled impulse-based TNT equivalence was, at most, approximately 10%.
- Regarding the MR dependence on TNT equivalence, a weak trend in which TNT equivalence decreased around MR = 4 was observed. Also, no significant scale effect related to weight of propellants was found in this experiment. However, we believe these results were strongly influenced by the destruction behavior of the glass dewars.
- The peak heat radiation observed in the experiments was similar to that of C-4. Importantly, the peak heat radiation did not exceed the permissible irradiance at any measurement distance.

Moving forward, we plan to conduct experiments with heavier propellants to reduce the influence of dewar destruction behavior and more accurately analyze the scale effect of weight of propellants.

Acknowledgements

The experiment was conducted with the support of IHI AEROSPACE Co., Ltd., SE LLC and OKUIGUMI Co., Ltd. We would like to express our gratitude for their support and cooperation.

References

[1] JAXA. 2019. Safety Regulation for Launch Site Operation, JERG-1-007E(E).
[2] Baker, W.E. 1973. Explosion in Air. University of Texas, Austin. 150-163.
[3] Kinney, G. F. 1962. Explosive Shocks in Air. McMillan Co., N.Y.
[4] Swisdak, M. M. 1975. Explosion Effects and Properties Part I - Explosion Effects in Air. NSWC/WOL/TR 75-116. Naval Surface Weapon Center, MD.
[5] Kingery, C. N. and Pannill, B. F. 1964. Peak Overpressure vs. Scaled Distance for TNT Surface Bursts (Hemispherical Charges). BRL Memorandum Report 1518.
[6] Kingery, C. N. and Bulmash, G. 1984. Airblast Parameters from TNT Spherical Air Bursts and Hemispherical Surface Bursts. ARBRL-TR-02555.
[7] Osipov, V., et al. 2013. Explosion hazard from a propellant-tank breach in liquid hydrogen-oxygen rockets. Journal of Spacecraft and Rockets, 50(4), 860-871.
[8] Kim, D., Kakudate, Y. and Usuba, S. 2017. Ignition by a collision of LOX and LNG. Science and technology of energetic materials, 78(1), 27-30.
[9] Blackwood, J. M., et al. 2023. An Interim Set of TNT Curves for LOX/LNG Explosions. 12th International Association for the Advancement of Space Safety (IAASS) Conference.
[10] Kundu, R. and Bangham, M. 2022. Explosive testing of cryogenic propellant mixtures. AIAA AVIATION 2022 Forum.
[11] Berkowitz, A. and Titulaer, S. 2024. Development of a Lox/Methane intact impact yield curve for a new launch vehicle. Journal of Space Safety Engineering, 11(4), 590-604.
[12] Willoughby, A. B., Wilton, C. and Mansfield, J. 1968. Liquid propellant explosive hazards. Volume I Technical Documentary Report, 126-139.
[13] Swisdak, M. M. 1994. Simplified Kingery airblast calculation. Arlington: Naval Surface Warfare Center.
[14] Headquarters, Dept. of the Army. 1965. Fundamentals of Protection Design. TM 5-855-1.
[15] Hannum, J. A. E. (ed). 1984. Hazards of Chemical Rockets and Propellants. Vol. III. Liquid Propellants., CPIA pub. no. 394, CPIA, The Johns Hopkins University, Applied Physics Laboratory, Laurel, Maryland.
[16] NASA. 2018. Safety Standard for Explosives, Propellants, and Pyrotechnics. NASA-STD-8719.12.